NASA/TM—2007-215039 AIAA–2007–5739

Further Characterization of an Active Clearance Control Concept

Shawn C. Taylor
The University of Toledo, Toledo, Ohio

Bruce M. Steinetz
Glenn Research Center, Cleveland, Ohio

Jay J. Oswald
J&J Technical Solutions, Cleveland, Ohio

December 2007

NASA STI Program . . . in Profile

Since its founding, NASA has been dedicated to the advancement of aeronautics and space science. The NASA Scientific and Technical Information (STI) program plays a key part in helping NASA maintain this important role.

The NASA STI Program operates under the auspices of the Agency Chief Information Officer. It collects, organizes, provides for archiving, and disseminates NASA's STI. The NASA STI program provides access to the NASA Aeronautics and Space Database and its public interface, the NASA Technical Reports Server, thus providing one of the largest collections of aeronautical and space science STI in the world. Results are published in both non-NASA channels and by NASA in the NASA STI Report Series, which includes the following report types:

- TECHNICAL PUBLICATION. Reports of completed research or a major significant phase of research that present the results of NASA programs and include extensive data or theoretical analysis. Includes compilations of significant scientific and technical data and information deemed to be of continuing reference value. NASA counterpart of peer-reviewed formal professional papers but has less stringent limitations on manuscript length and extent of graphic presentations.

- TECHNICAL MEMORANDUM. Scientific and technical findings that are preliminary or of specialized interest, e.g., quick release reports, working papers, and bibliographies that contain minimal annotation. Does not contain extensive analysis.

- CONTRACTOR REPORT. Scientific and technical findings by NASA-sponsored contractors and grantees.

- CONFERENCE PUBLICATION. Collected papers from scientific and technical conferences, symposia, seminars, or other meetings sponsored or cosponsored by NASA.

- SPECIAL PUBLICATION. Scientific, technical, or historical information from NASA programs, projects, and missions, often concerned with subjects having substantial public interest.

- TECHNICAL TRANSLATION. English-language translations of foreign scientific and technical material pertinent to NASA's mission.

Specialized services also include creating custom thesauri, building customized databases, organizing and publishing research results.

For more information about the NASA STI program, see the following:

- Access the NASA STI program home page at *http://www.sti.nasa.gov*

- E-mail your question via the Internet to *help@sti.nasa.gov*

- Fax your question to the NASA STI Help Desk at 301–621–0134

- Telephone the NASA STI Help Desk at 301–621–0390

- Write to:
  NASA Center for AeroSpace Information (CASI)
  7115 Standard Drive
  Hanover, MD 21076–1320

NASA/TM—2007-215039 AIAA–2007–5739

Further Characterization of an Active Clearance Control Concept

Shawn C. Taylor
The University of Toledo, Toledo, Ohio

Bruce M. Steinetz
Glenn Research Center, Cleveland, Ohio

Jay J. Oswald
J&J Technical Solutions, Cleveland, Ohio

Prepared for the
43rd Joint Propulsion Conference
sponsored by the American Institute of Aeronautics and Astronautics
Cincinnati, Ohio, July 8–11, 2007

National Aeronautics and
Space Administration

Glenn Research Center
Cleveland, Ohio 44135

December 2007

Acknowledgments

The authors wish to acknowledge Richard Tashjian for his contributions toward rig setup and continuous support during testing.

Level of Review: This material has been technically reviewed by technical management.

Available from

NASA Center for Aerospace Information
7115 Standard Drive
Hanover, MD 21076–1320

National Technical Information Service
5285 Port Royal Road
Springfield, VA 22161

Available electronically at http://gltrs.grc.nasa.gov

Further Characterization of an Active Clearance Control Concept

Shawn C. Taylor
The University of Toledo
Toledo, Ohio 43606

Bruce M. Steinetz
National Aeronautics and Space Administration
Glenn Research Center
Cleveland, Ohio 44135

Jay J. Oswald
J&J Technical Solutions
Cleveland, Ohio 44135

Abstract

A new test chamber and precision hydraulic actuation system were incorporated into an active clearance control (ACC) test rig at NASA Glenn Research Center. Using the improved system, a fast-acting, mechanically-actuated, ACC concept was evaluated at engine simulated temperatures and pressure differentials up to 1140 °F and 120 psig, on the basis of secondary seal leakage and kinematic controllability. During testing, the ACC concept tracked a simulated flight clearance transient profile at 1140 °F, 120 psig, with a maximum error of only 0.0012 in. Comparison of average dynamic leakage of the system with average static leakage did not show significant differences between the two operating conditions. Calculated effective clearance values for the rig were approximately 0.0002 in. at 120 psig, well below the industry specified effective clearance threshold of 0.001 in.

Nomenclature

ϕ	Flow Factor, $\frac{\left(\text{lbm/s}\sqrt{°R}\right)}{\text{psia}}$
X	Distance between the inner diameter of the face seal and inner edge of the flexure seal, in.
δ_{flow}	Effective clearance where flow is choked, in.
A_{flow}	Area where flow is choked, in.^{2}
C	Circumference of seal test section, in.
$\dot{m}$	Measured mass flow rate, lbm/s
R	Gas constant for air, 53.3 lbf-ft/lbm-°R
T	Temperature, °R
g_c	Gravitational constant, 32.2 lbm-ft/lbf-s^2
P_s	Supply pressure, psia

Introduction

Previous investigations of a fast-acting, mechanically-actuated, active clearance control (ACC) concept at NASA Glenn Research Center (GRC) highlighted the feasibility of monitoring and regulating blade tip clearance in the high pressure turbine (HPT) section of modern gas turbine engines (refs. 1 to 3). These investigations, completed using the non-rotating ACC test rig at NASA GRC, evaluated an ACC concept on the basis of dynamic controllability, secondary seal leakage, and overall kinematic performance. Upper load capacities of the electric stepper motors used for actuating simulated blade-tip

clearances limited dynamic leakage testing of the ACC system to a maximum chamber pressure of 30 psig. To extend testing capabilities to the full 120 psig design pressure, a servo-hydraulic actuation package was implemented into the ACC test system. In addition, a new test chamber was installed to correct imperfections that occurred during the fabrication of the original test chamber. This study examines the performance capabilities of the new servo-hydraulic actuators, as well as those of the ACC concept as a whole with the new actuation system and redesigned test chamber in place.

A. Background

Figure 1 is a cross section of the combustor and two-stage HPT of a modern gas turbine engine which shows the location of the HPT blade tip seal (ref. 4). Blade tip seals line the inner circumference of the stationary engine case to form a shroud around the rotating turbine blades and limit the amount of gas that spills over the tips. Clearance between the blade tips and the sealing shroud varies both with engine operating condition (e.g., ground idle, take-off, cruise, decel, etc.) and service duration. These operating condition clearance variations are produced by flight loads applied to engine structures (both static and rotating) and by engine component wear. A fast-acting, active tip clearance control concept was designed by Lattime, et al. (ref. 5), to stabilize and regulate varying blade tip clearances. This concept accommodates even worst case clearance transients, such as those occurring during a “stop-cock” event where an engine would be shut down in flight, allowed to windmill, and then be restarted to full power. The ACC concept was incorporated into a test rig at NASA GRC (fig. 2) and evaluated at multiple temperatures and pressure differentials on the basis of secondary seal leakage, dynamic controllability, and overall kinematic performance (refs. 1 to 3). Preliminary evaluations of the ACC concept, however, could not be extended to the full operating conditions of 1200 °F and 120 psig chamber pressure as designed. Upper load limits of the stepper motors (~500 lbf maximum capacity) used to adjust simulated clearances in the test rig prevented dynamic testing at pressures above approximately 30 psig because the motors were unable to support corresponding pressure generated loads. Operating temperatures were generally limited to 1000 °F after imperfections in the positioning welds of the test chamber actuator rod tubes (fig. 3) were discovered during hydrostatic testing. These welds were determined to be non-critical to test chamber structural integrity, but to add extra safety margin, temperature exposure above 1000 °F was limited until corrective measures could be taken.

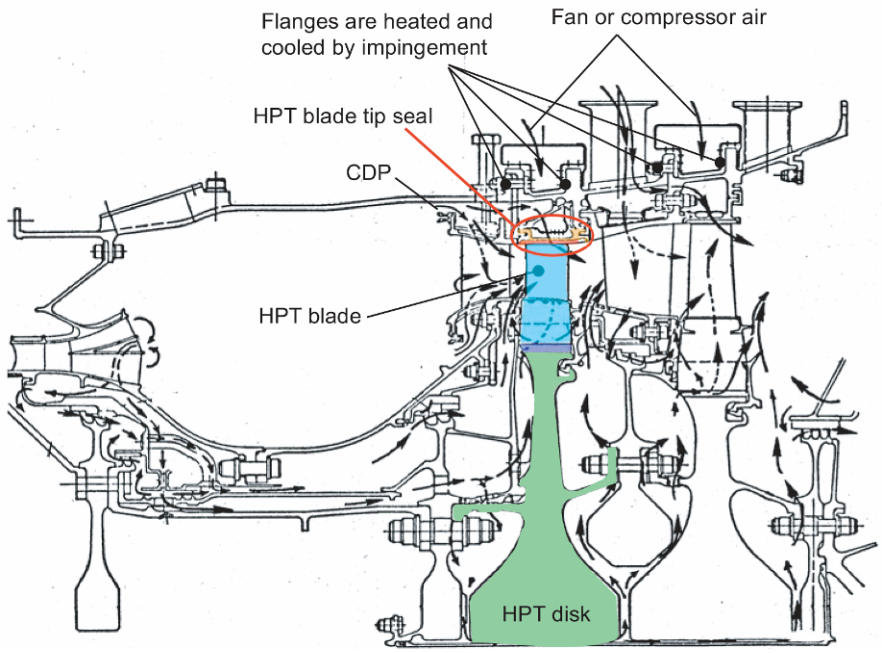

Figure 1.—HPT blade tip seal location in a modern gas turbine engine (ref. 4).

Figure 2.—Photograph of the active clearance control system.

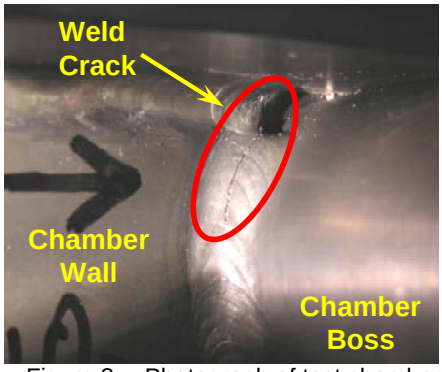

Figure 3.—Photograph of test chamber boss positioning weld crack.

B. Benefits of Active Clearance Control (ACC)

Integrating a fast-acting, mechanically-actuated, ACC concept into the HPT would consistently reduce blade clearance, decrease the amount of air spilling over the blade tips, and therefore increase turbine efficiency. Reduced blade tip clearances would allow the engine to satisfy thrust and performance needs at lower operating temperatures, with less fuel burn, and decreased rotor inlet temperatures. Lower operating temperatures would increase the service life of internal hot section components and extend engine operating time between overhauls. A tip clearance reduction of 0.010 in. would decrease exhaust gas temperature (EGT) by approximately 10 °C (ref. 6). Deterioration of the EGT margin is the primary parameter used to determine when an engine is removed from service. The same 0.010 in. tip clearance reduction would decrease specific fuel consumption by 0.8 to 1 percent, and lower NO_x, CO, and CO_2 emissions (ref. 6). Other benefits would include enhanced payload and mission range capabilities. Additional benefits of advanced active clearance control systems are discussed in the works by Lattime, et al., (ref. 6) General Electric (ref. 7), and Wiseman and Guo (ref. 8).

C. Objectives

This investigation builds on previous work that characterized the behavior of the ACC concept at both room and elevated temperatures (refs. 1 to 3). Test rig limitations identified during those studies have been addressed through the integration of a new servo-hydraulic actuation package and a new test chamber pressure vessel with existing ACC test hardware. Utilizing these improvements, the goals of this investigation were to:

- Characterize the accuracy and repeatability of the new servo-hydraulic actuators (individually) before incorporating them into the ACC test system.
- Characterize ACC system secondary seal leakage (both static and dynamic) up to the full design pressure and temperature of 120 psig and 1200 °F, respectively, while using the new servo-hydraulic actuation system to simulate engine clearance control.
- Evaluate the ability of the ACC system to track simulated take-off clearance transient profiles (at pressures and temperatures up to 120 psig and 1200 °F) using the new servo-hydraulic actuators.

II. Test Facility and Procedures

A. Test Hardware

1. Test Rig Overview

The ACC test rig (fig. 4) was designed to simulate the temperature and pressure conditions of the environment surrounding the backside of the turbine shroud segments. This rig is used to evaluate clearance control systems in a “static" environment without blade rotation. Rig specifications were selected based on current engine requirements. Table 1 compares the main characteristics of the ACC test rig to a typical modern high bypass ratio engine.

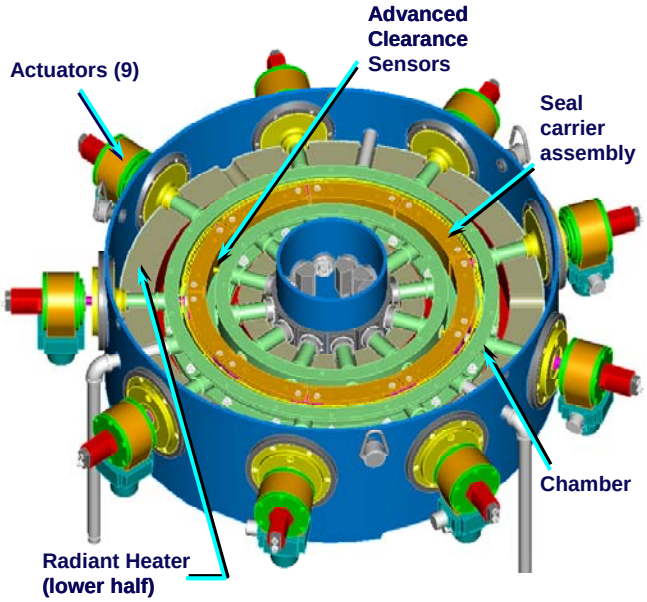

Figure 4.—ACC test rig with housing lid and chamber cover plate removed for clarity (ref. 5).

TABLE 1.—COMPARISON OF ACC RIG DESIGN TO THE OPERATING CHARACTERISTICS OF A TYPICAL MODERN HIGH BYPASS RATIO ENGINE

Parameter	ACC rig design	Reference engine
Shroud backside pressure (psia)	135	500
Pressure differential (psid)	120	150
Shroud Backside temperature		
Current (°F)	1200	950 to 1250
Future (°F)	1250 to 1300	1250 to 1300
Diameter (in.)	20	30
Shroud face width (in.)	2	2
Number of shrouds/seal carriers	9	16
Pressure induced load on actuator (at pressure differential) (lbf)	1650	1750
Nominal clearance change (e.g., stroke) (in)	0.190	0.050
Clearance change rate (in./sec)	0.01	0.01
Clearance measurement technique		
Current	Capacitance	Not used
Future (under development)	Microwave	Capacitance/ microwave

The Inconel 718 (Special Metals Corp., Huntington, WV) seal carrier assembly shown in figures 4 and 5 is a concept that would be used in a turbine to support the tip seals that surround the rotor. The assembly consists of nine individual seal carrier arc segments that are connected through a series of Inconel 718 “links” (fig. 5) to form a circular shroud. One connection between the link and carrier is a pinned joint, and the other is a slotted joint. Each link (9 total) is rigidly connected to an Inconel 718 actuator rod which is attached to a servo-hydraulic actuator that provides the radial motion needed to control simulated blade tip clearance. This kinematic arrangement allows for dilation of the seal carrier shroud when the actuator rods are moved radially outward and contraction when they are moved inward. Dilation of the seal carrier shroud increases simulated tip clearance, and contraction decreases clearance. Actuator control is implemented through National Instruments motion controllers and a series of algorithms coded in LabVIEW (National Instruments Corp., Austin, TX). Details of ACC test rig control system are presented by Steinetz, et al (ref. 1).

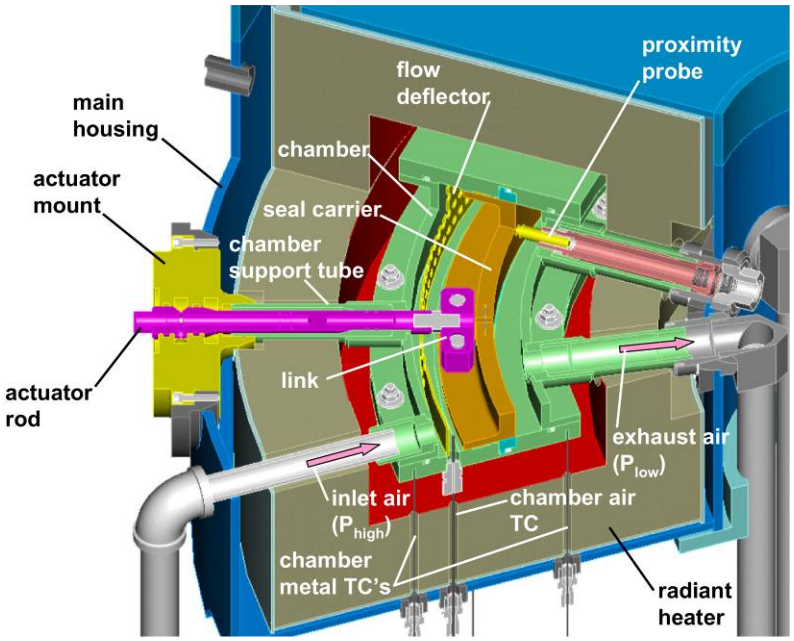

Figure 5.—ACC cut-away showing detail for one of nine actuator rods, an attachment link, actuator mount, seal carriers, proximity probe clearance sensor, inlet air supply pipe, air flow directions, and radiant heater (ref. 5).

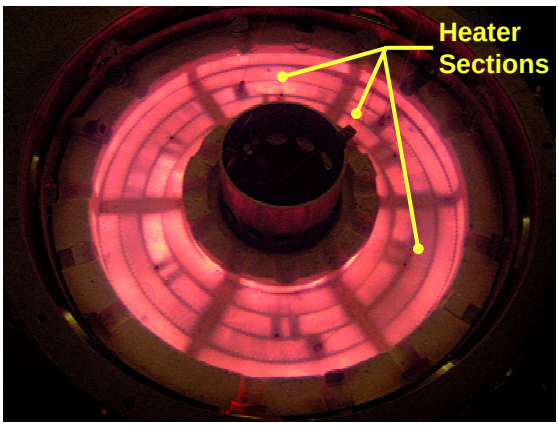

Figure 6.—Photograph of the radiant heater at temperature with the test chamber removed highlights the heater's six sections, each of which can be independently controlled.

The seal carrier shroud is encased in a test chamber that is used to create the temperature (T3) and pressure (P3) conditions typical of the environment behind the blade tip seals in an actual HPT. The test chamber consists of an upper and lower cover plate, and inner and outer walls (fig. 5). Hot, high-pressure air is supplied to the backside of the seal carrier shroud through three penetrations of the outer chamber wall. The hot air (heated by two 35 kW inline air heaters stacked in series) heats the inside of the test chamber and is the medium for evaluating seal leakage. The outside of the test chamber is heated by the upper and lower halves of a split annular radiant heater (figs. 5 and 6). Combined, these two systems provide the heat needed to simulate the T3 environment. Additional detail of the ACC heater systems is provided by Lattime, et al (ref. 5).

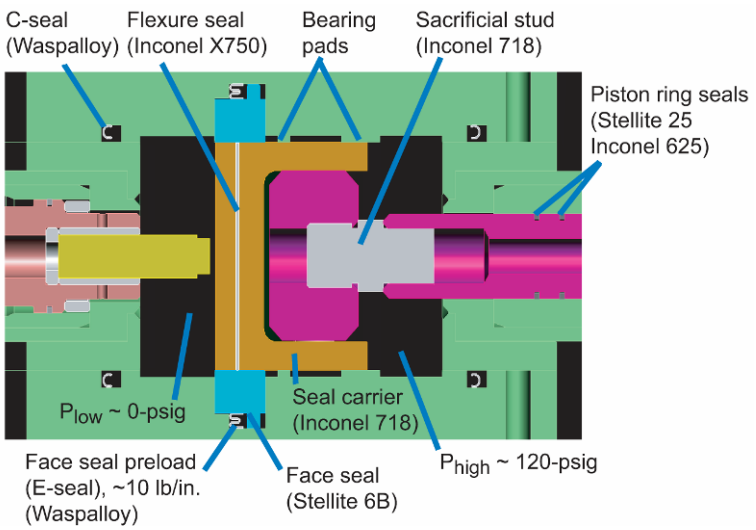

Figure 7.—Chamber cutaway highlighting the ACC system secondary seals and their respective materials.

2. Secondary Seals

To maintain a significant positive backpressure and create the desired P3 pressure differential across the seal carrier shroud, multiple secondary seals are required. These seals are highlighted in figure 7. The top and bottom of the seal carrier shroud are sealed with face seals (Stellite 6b (Deloro Stellite Co., Goshen IN)) secured in grooves in the upper and lower chamber cover plates and preloaded by E-seals (Waspaloy (Haynes International, Inc., Kokomo, IN)). The flow path between the individual seal carriers is blocked by thin, pressure activated flexure (spline) seals (Inconel X-750 (Special Metals Corp., Huntington, WV)). The flexure seals are inserted into precision slots machined into the ends of the seal carriers. When the test chamber is pressurized, the faces of the flexure seals seat on the low pressure side of the mounting slot (radially inward side) and seal along their top and bottom edges with the face seals. Since the flexure edges must mate with the face seals to sustain a backpressure, the stroke length of the rig's actuation system is governed by the width of the face seals. The center of this stroke (flexure seals in the center of the face seals) is referenced as the nominal “home” position of the seal carrier shroud. Waspaloy C-seals are used to prevent leakage between the test chamber cover plates and the chamber wall flanges. Piston ring seals (Stellite 25 (Deloro Stellite Co., Goshen IN) and Inconel 625 (Special Metals Corp., Huntington, WV)) are used to minimize flow past the actuator rod and air supply locations. Additional information on the design of the test chamber and seal components is given by Lattime, et al., (ref. 5) and representative component leakage levels for each seal at room temperature are presented by Steinetz, et al. (ref. 1).

3. Instrumentation

Simulated clearance values are continuously monitored during testing with four capacitance-based proximity probes. Three probes are positioned at 90° intervals and the fourth probe is offset from the nearest adjacent probe by 30°. Probe details are listed in table 2. Leakage values are collected using one of two mass flow meters. Specifications for the flow meters, pressure transducers, and thermocouples used to monitor the ACC test environment are provided in table 3.

TABLE 2.—CAPACITANCE CLEARANCE PROBE SPECIFICATIONS

Calibrated operating maximum temperature	1500 °F
Measurement range (in.)	0 to 0.125
Accuracy (in.)	0.0002
Resolution (in.)	0.00005
Excitation voltage (V)	15
Probe diameter (in.)	0.375
Weight (lbs)	0.04
Manufacturer	Capacitec
Model no.	HPC 150

TABLE 3.—INSTRUMENTATION SPECIFICATIONS

Thermocouples	Type K
Manufacturer	Omega
Accuracy (°F)	± 4
Range (°F)	–328 to 2282
Pressure Transducers	
Manufacturer	Druck
Model	PMP4010
Accuracy (psi)	0.12
Range (psig)	0 to 300
Flow Meters	
Manufacturer	Teledyne Hastings
Models	HFM 301; HFM 306
Accuracy (lbm/s)	0.0003; 0.0042
Range (lbm/s)	0.0355; 0.1857

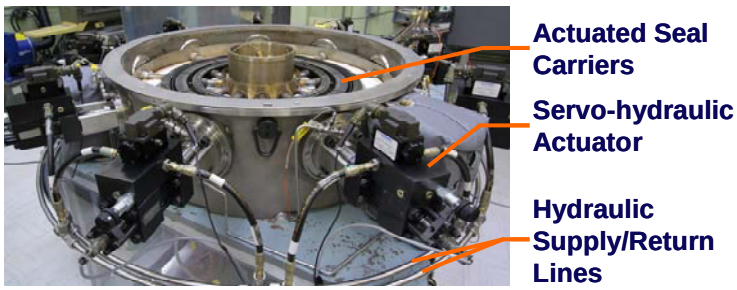

Figure 8.—Photograph of the new servo-hydraulic actuators installed on the test rig.

TABLE 4.—SERVO-HYDRAULIC ACTUATOR SPECIFICATIONS

Hydraulic cylinder	
Manufacturer	Eaton
Model	TJ-TZXX Series
Bore and rod	2-in. bore, 1-in. dia. double rod
Pressure range (psi)	200-3000
Stroke (in.)	0.2
Servo valve	
Manufacturer	Vickers
Model	SM4-10(1)3.8-80/40-10
LVDT	
Manufacturer	Schaevitz
Model	HCA-250
Range (in.)	±0.250
Linearity (% Full Range)	±0.20

4. Hydraulic Actuators

For this investigation, seal carriers were actuated using a servo-hydraulic actuation system that consists of nine individual servo-hydraulic actuators (fig.8) energized by a central hydraulic power unit (HPU). System specifications are presented in table 4. These actuators are conventional off-the-shelf items that were selected for their ability to satisfy design requirements and fit within the project budget; smaller, lighter weight actuators would be used in actual engine applications.

Figure 9.—Photograph showing frost on the new test chamber outer wall just after the shrink fit installation of an actuator support tube.

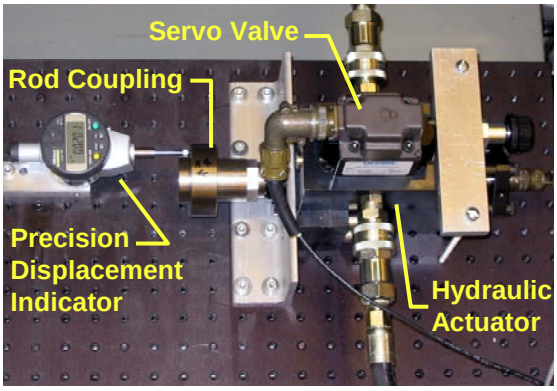

Figure 10.—Photograph of the setup used to bench test the servo-hydraulic actuators prior to acceptance and system installation.

5. Improved Test Chamber

Building on lessons learned from the first generation ACC test chamber, new inner and outer chamber walls were designed and fabricated to enable system operation at full design capacity of 120 psig at 1200 °F. To avoid the possibility of a reoccurrence of the weld issues experienced during the fabrication of the first generation chamber, new inner and outer walls were machined from a solid plate of Inconel 718. Actuator support tubes and chamber exhaust ports were installed directly into the walls using a shrink-fit technique (fig. 9). This technique used a liquid nitrogen bath to cool the support tubes and exhaust ports, shrinking them enough that an average interference fit of 0.001 in. between the walls and the inserted parts was achievable through hand assembly. The new chamber design eliminated the need for welds, is much more robust, and can more easily accommodate future actuation and sealing concepts for evaluation in the ACC test rig.

B. Procedures: Actuator Testing

1. Benchtop Evaluation

Each of the nine individual servo-hydraulic actuators was evaluated using a bench-top test fixture to verify its compliance with required accuracy and hysteresis prior to being installed on the ACC test rig. The experimental setup used to evaluate actuator accuracy and hysteresis is presented in figure 10. As shown in the figure, each actuator was secured to a precision test platform and a digital displacement gage (±0.00012 in. accuracy) was positioned so as to align its plunger coaxially with the actuator rod. The actuator rod was then fully retracted and the displacement gage was zeroed. From that position, the actuator was commanded to move incrementally (0.010 in. steps) across a stroke range of 0.180 in. With each increment, a displacement was recorded from the digital gage (actual position) for comparison with the commanded position. Once the end of the stroke length was reached, actuation direction was reversed and the rod was retracted across the same series of commanded positions. Using the collected data, accuracy was determined by subtracting target positions from the actual position readings, and hysteresis error was determined by subtracting the two actual positions (outward stroke minus inward stroke)

corresponding to each commanded position. Design requirements established an error tolerance band of ±0.0003 in. for both actuator accuracy and hysteresis.

2. On-Rig Evaluation

To help quantify accuracy and controllability improvements achieved through the addition of the new ACC servo-hydraulic actuation system, an on-rig test was conducted to evaluate pressure induced seal carrier deflection. This evaluation incorporated a combination of dead band in the actuators, elastic deformation of the actuator rods and connecting hardware, deflection of actuator seals, as well as any other sources of compliance that may exist within the assembly. Individual contributions to total pressure induced seal carrier deflection were not of immediate concern.

To perform the test, the seal carriers were placed in range of the capacitance probes while the test chamber was not pressurized, and clearance readings from the four probes were recorded. Without moving the actuators, the chamber pressure was increased in 20 psi increments to full pressure capacity (120 psig), and then returned to 0 psig, retracing the same intervals. At each step, corresponding chamber pressure and clearance values were recorded. Pressure induced deflections were calculated for all four probe locations by subtracting the clearance at each elevated pressure level from the initial clearance at ambient pressure. In addition to deflection, hysteresis during this procedure was evaluated as the difference between the two clearance values collected at each chamber pressure (one during pressure increase, one during pressure decrease).

C. Procedures: Elevated Temperature Evaluation

1. General Background

Previous testing of the ACC rig evaluated its performance up to 1000 °F, examining controllability, static leakage rates at chamber pressures up to 120 psig, and dynamic leakages to chamber pressures of approximately 30 psig (ref. 3). Using those test procedures as a foundation, test plans were developed to characterize rig performance up to full system temperature and pressure utilizing the newly installed servo-hydraulic actuation system.

Before the system was heated, the seal carriers were centered about the rig's central axis in range of the capacitance probes. The actuators were then set to closed-loop control, enabled, and commanded to maintain a constant arbitrary simulated clearance value. With this procedure, the system used feedback from the capacitance probes during heatup to compensate for thermal expansion and prevent undesired interference between its internal components.

The radiant and air heaters were ramped at approximately equal rates (nominally 50 °F/min.) to avoid the formation of significant thermal gradients across the test section and to promote uniform expansion of the rig's internal components. Due to the large thermal mass of those components, actual metal heating rates were somewhat slower than the nominal value. Before testing was initiated, the rig was subjected to a heat soak interval to allow internal temperatures to equalize at the desired test temperature.

Target test conditions for the evaluations contained herein included temperatures of 600 °F, 950 °F, and 1200 °F, and pressure differentials ranging from 60 to 120 psig. A positional parameter, X, was defined to describe the position of the seal carriers and flexure seals relative to the face seals. X, shown graphically in figure 11, is the distance from the inner diameter of the face seal to the inner edge of the flexure seal when it is installed in its slot in the seal carrier (ref. 3). X accurately describes seal carrier position by accounting for motion resulting from mechanical actuation, pressure induced displacements, and thermal expansion of sealing components and surrounding support structures. Using this information, meaningful leakage comparisons can be made across varied test conditions (temperature, chamber pressure, etc.). At the nominally defined "home" position of the sealing shroud, the flexure seals are at the centerline of the face seal surface (X = 0.250 in.). Radially outward seal carrier motion increases the value of X, and inward motion decreases it.

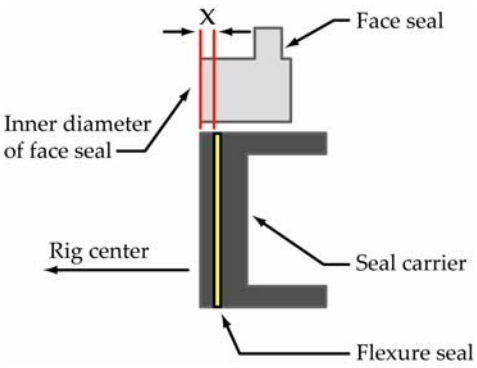

Figure 11.—Graphical depiction of the X parameter.

2. Static Leakage Evaluation

To begin the evaluation, the test rig was heated to the prescribed test temperature, the chamber pressure was adjusted to the desired level, and the seal carrier assembly was actuated radially inward until the minimum measured clearance (relative to the capacitance probes) reached approximately 0.005 in. From that position, the seal carriers were moved radially outward, stopping incrementally (~0.010 in. steps) to collect static leakage values, until the outward stroke limit was reached. Due to rig component thermal expansion, stroke range limits varied with test temperature (higher temperature tests had less available stroke than those at lower temperatures). When the outward stroke limit was reached, actuation was reversed, and the seal carriers retraced the same stopping positions covered during the outward stroke. After a stroke cycle was completed, the chamber pressure was adjusted, and the process was repeated until all pressures of interest were evaluated. This procedure facilitated an evaluation of the effects of temperature, pressure differential, radial seal position (X), and direction of seal carrier motion (radially inward vs. outward) on static ACC system leakage.

3. Dynamic Leakage Evaluation

Dynamic leakage data was collected using the same test procedures and conditions utilized for static leakage testing; however, the seal carriers were not intermittently stopped, they were actuated continuously across the available stroke range. At each temperature and pressure combination, leakage data was continuously logged at a rate of 0.4 Hz while the seal carriers were in motion. Seal carrier actuation rates of 0.001 in./sec and 0.005 in./sec were evaluated.

4. Tracking of a Simulated Flight Clearance Transient Profile

The ability of the ACC system to track actual engine clearance transients while at elevated temperatures and pressures was evaluated by examining the system's ability to track a mission simulated clearance vs. time profile streamed to the hydraulic actuator control system. The profile used in this study is representative of the clearance transient present during takeoff in large commercial turbine engines. The profile is 200 seconds long and includes a 0.045 in. clearance change over a period of 10 seconds. Simulated clearances are regulated using a two-level closed-loop control scheme incorporated into the hydraulic actuator control system. The outer level control loop continuously monitors the readings of the system's four capacitance probes, and compares the minimum measured clearance to the set point specified by the simulated profile. Data from that comparison is then relayed to the inner control loop, which contains the actuator LVDT's, and the positions of the nine actuators are modified to satisfy clearance changes requested by the outer loop. Using the minimum clearance reading for controlling the system is a conservative approach that was implemented to prevent the occurrence of blade rubs in an actual engine. System performance during this evaluation was quantified in the form of positional error which was calculated as the difference between the commanded clearance value and the minimum clearance measured by the capacitance probes.

III. Results and Discussion

A. Actuator Testing

1. Benchtop Evaluation

Bench testing of the individual hydraulic actuators showed that they easily satisfied the design requirements that established a positional accuracy and hysteresis error tolerance of ±0.0003 in. for use with the ACC test rig. Representative data from these tests is presented in figures 12 and 13. The largest noted positional error had a magnitude of 0.0002 in. and the largest hysteresis error had a magnitude of 0.0001 in.

2. On-Rig Evaluation

The maximum pressure induced deflection (average of four probes) observed in this test was 0.0068 in. at a chamber pressure of 120 psig, and the maximum hysteresis was 0.0013 in. Previous tests using first generation stepper motor actuators showed a pressure induced seal carrier deflection as large as 0.022 in. (115 psig chamber pressure), and a maximum hysteresis of 0.0042 in. A comparison of the two data sets is presented in figure 14. The integration of the servo-hydraulics package reduced observed pressure induced deflection and hysteresis by approximately 69 percent. This improvement is attributed to the increased overall "stiffness" and load bearing capabilities of the servo-hydraulic system. By decreasing pressure induced deflection, the overall accuracy and controllability of the ACC system is significantly enhanced. It is important to note that the effects of pressure induced deflection are only a concern if the ACC system is run in "open loop" control. By switching to "closed loop" control, the actuation system uses feedback from the capacitance probes to stabilize simulated clearances, and the error associated with pressure induced seal carrier compliance is eliminated.

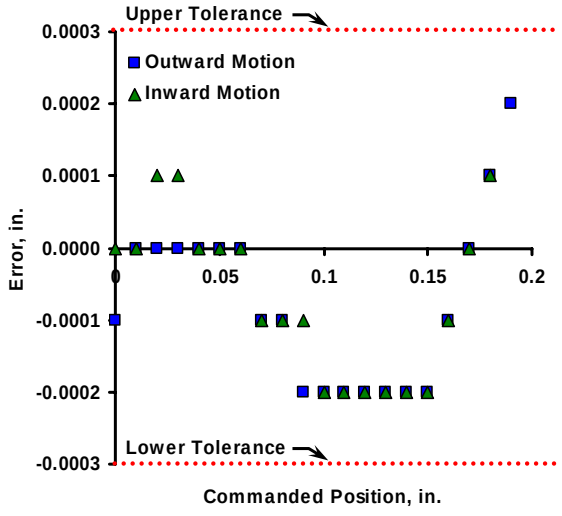

Figure 12.—Plot showing actuator positional error as a function of commanded position.

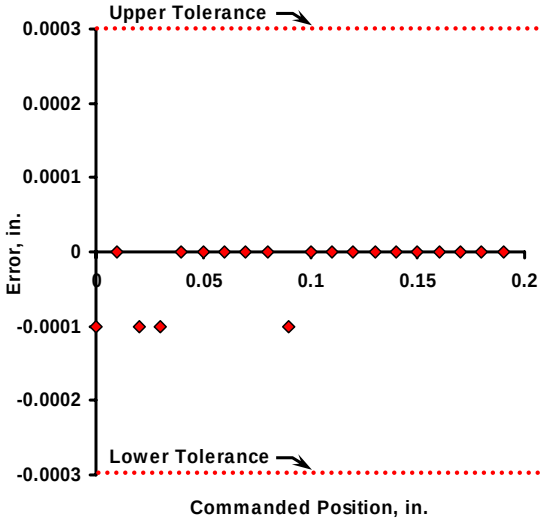

Figure 13.—Plot showing actuator hysteresis error as a function of commanded position.

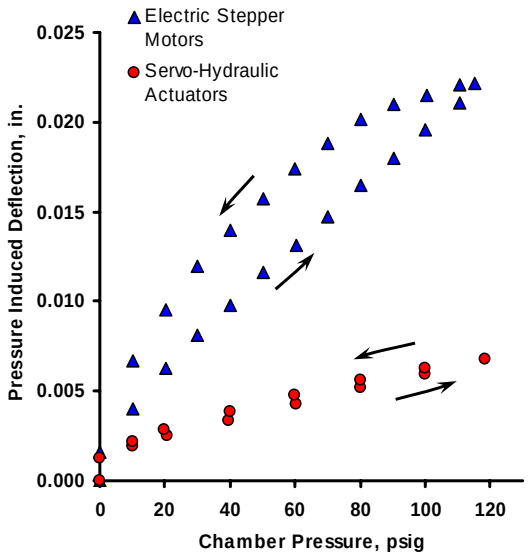

Figure 14.—Plot comparing pressure induced seal carrier deflections for ACC servo-hydraulic and electric stepper motor actuation systems.

B. Elevated Temperature Evaluation

High temperature tests were conducted at temperatures that deviated slightly from the planned target values. Average test temperatures included 630, 945, and 1140 °F. The target design temperature of 1200 °F was not reached because system secondary seals performed so well at full chamber pressure and maximum heater capacity that leakage was low enough that the air flow through the system was insufficient to carry the heat from the heating elements to the chamber inlets without heat loss to the surrounding environment. Researchers are investigating whether more effective insulating techniques could be used to further minimize the temperature drop between the air heater outlet and the rig inlets.

The targeted test pressure range also required modification from its original span. At test temperatures above 630 °F, only pressures of 100 and 120 psig could be achieved. At 100 psig, corresponding leakage rates were so low that any further pressure decrease risked a condition of insufficient air flow across the heater elements which could result in heater failure.

1. Static Leakage Evaluation

As observed in previous studies (refs. 2 and 3), seal leakage values collected during an inward actuator stroke were consistently lower than those collected during an outward stroke. Decreased leakage while the seal carriers were moving inward was attributed to a pressure induced roll of the face seals that resulted in higher contact loads at the seals' outer edges that "pinch" the seal carriers (ref. 2). During inward motion of the seal carriers, it is believed that frictional force between the face seal outer edges and the seal carrier surfaces intensifies the pinching action, thus decreasing effective flow area and reducing overall system leakage. Outward motion of the seal carriers is believed to reduce the pinching action of the face seals, resulting in a larger flow area and increased mass flow rates. Leakage vs. position data is presented for all three test temperatures at 120 psig in figures 15 to 17. At 630 °F, leakage values collected during an inward stroke were an average 19 percent lower than those collected during an outward stroke. The maximum leakage rate at 630 °F was 0.0304 lbm/s, and the minimum was 0.0209 lbm/s. In the 945 and 1140 °F tests, leakages collected during inward strokes were 19 and 20 percent lower, respectively, than corresponding leakages from outward strokes. The highest leakage observed at 945 °F was 0.0264 lbm/s and the lowest was 0.0186 lbm/s. At 1140 °F, leakage ranged from 0.0218 to 0.0303 lbm/s. Observed leakages at lower pressure differentials had lower mass flow rates as

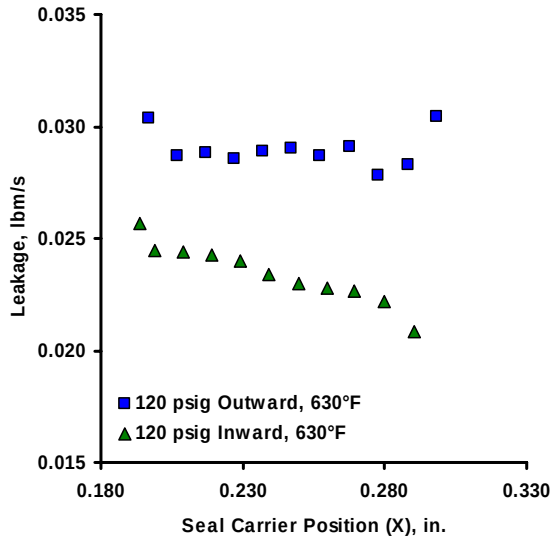

Figure 15.—Static leakage as a function of seal carrier position, X, and direction of motion at 120 psig, 630 °F.

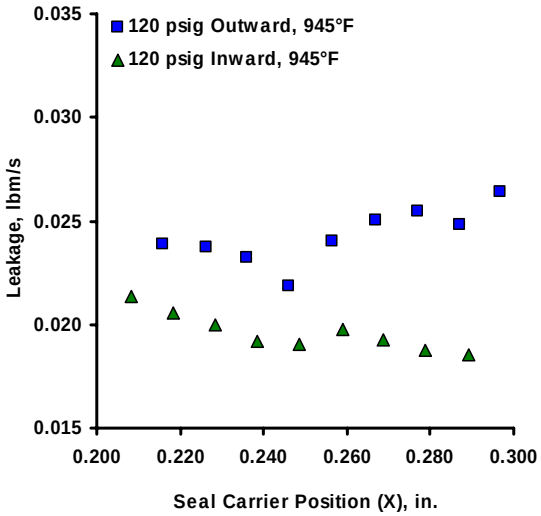

Figure 16.—Static leakage as a function of seal carrier position, X, and direction of motion at 120 psig, 945 °F.

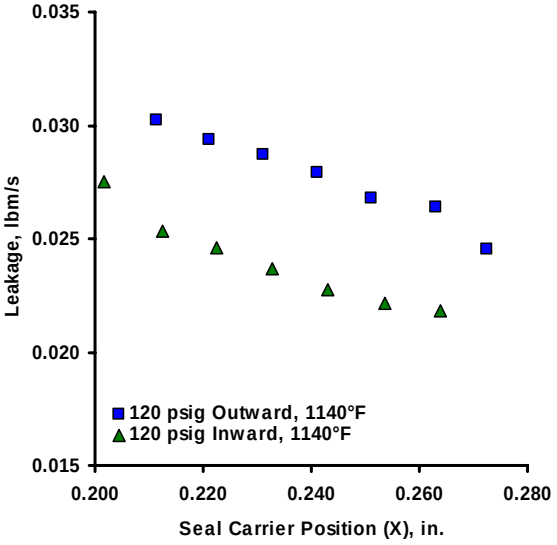

Figure 17.—Static leakage as a function of seal carrier position, X, and direction of motion at 120 psig, 1140 °F.

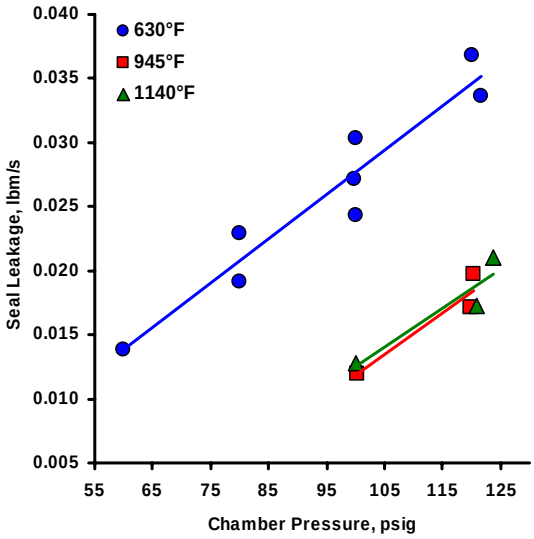

Figure 18.—Effect of chamber pressure on seal leakage with the seal carriers positioned at X = 0.257 in.

would be expected, but still followed similar trends as noted above. Leakage vs. pressure data at approximately the home position (X = 0.257 in.) is presented in figure 18.

To gain further insight into factors affecting rig leakage, a flow factor, ϕ, was calculated for leakage values at each of the test temperatures where the pressure differential was 120 psig, and the seal carriers were at approximately the "home" position (X = 0.250 in.). The flow factor, ϕ, accounts for variation in mass flow rate due to normal gas density effects, and is defined as:

$$\phi = \frac{\dot{m}\sqrt{T}}{P_s} \tag{1}$$

As shown in figure 19, flow factor changes with both temperature and direction of seal carrier motion when it was stopped at the home position. Flow factor values are an average 18 percent lower for leakage rates collected during an inward stroke of the actuators. As temperature was increased from 630 °F to 945 °F, the flow factors decreased for both the inward and outward strokes, 5.5 and 15.5 percent respectively; however, an additional temperature increase from 945 to 1140 °F increased the flow factors, 25 percent during the inward stroke, and 32 percent during the outward stroke. These observations, coupled with trends observed in raw leakage data, suggest that physical clearances inside the rig are changing as operating conditions are varied, and leakage changes cannot be explained by gas density effects alone.

2. Dynamic Leakage Evaluation

Evaluation of dynamic leakage revealed trends similar to those observed in the static leakage tests. Recorded leakage values were consistently lower while the actuators were moving radially inward. A representative data set from those evaluations is presented in figure 20. Leakage as a function of seal carrier position is plotted for the 1140 °F test at pressure differentials of both 100 and 120 psig, and a seal carrier actuation rate of 0.001 in./s. During the outward stroke, observed leakages are higher than those during the inward stroke. Inward stroke leakage (0.0231 lbm/s avg.) was 17 percent lower than the outward stroke (0.0277 lbm/s avg.) at 120 psig, and 21 percent lower at 100 psig (0.0176 lbm/s outward avg., 0.0139 lbm/s inward avg.).

Comparison of leakage values collected during actuation at 0.001 in./s to leakage data collected during 0.005 in./s actuation showed that the rate increase did not consistently affect the magnitude of observed leakage values (Fig. 21); however, data resolution was decreased during 0.005 in./s actuation due to sampling rate and settling time limitations of the flow meters used for these studies.

In figure 21, dynamic leakage at 120 psig for both actuation rates and all three test temperatures is compared to static leakage collected during similar test conditions. Given the ±0.0003 lbm/s accuracy of the mass flow meter used for the 1140 °F and 945 °F evaluations, and the ±0.0042 lbm/s accuracy of the flow meter used in the 630 °F tests, many of the observed differences between static and dynamic leakage fall within the flow meter error tolerance bands and are considered negligible. As the reader can clearly see in figure 21, there are no trends in the data that would suggest a consistent change in system leakage as the seal carriers are transitioned between static and dynamic states.

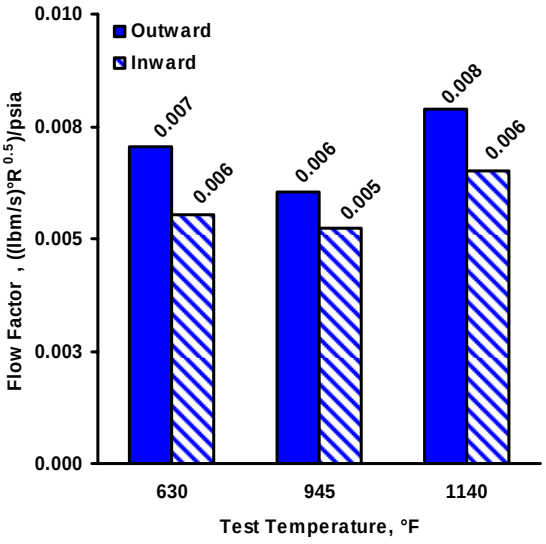

Figure 19.—Flow factor comparison for static leakages at the “home” position and 120 psig.

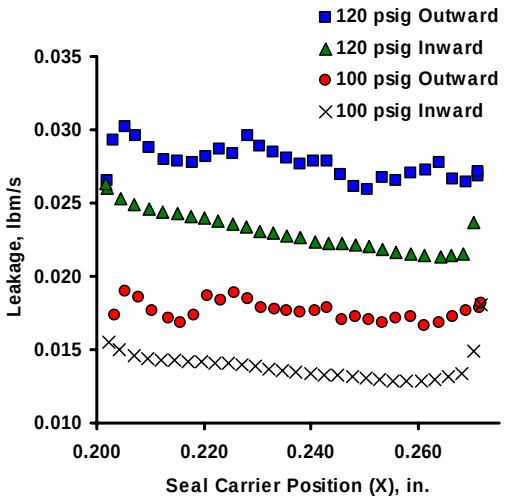

Figure 20.—Dynamic leakage as a function of seal carrier position, X, at 1140 °F and both 100 and 120 psig.

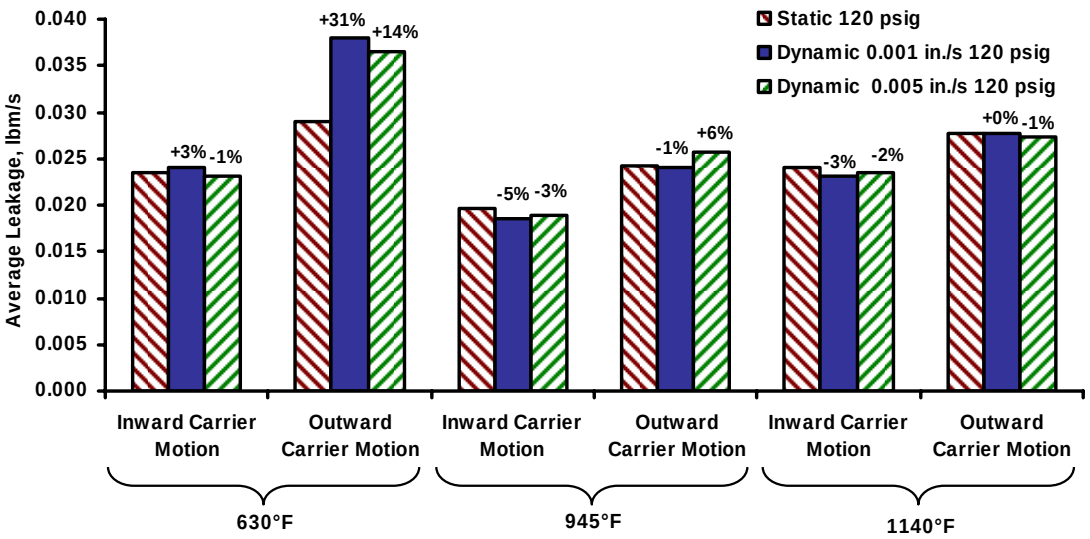

Figure 21.—Comparison of average dynamic leakage to average static leakage at 120 psig for the 630, 945, and 1140 °F tests.

3. Simulated Flight Profile Tracking

The installation of the new servo-hydraulic actuation package onto the ACC test rig enabled the system to easily track a simulated engine clearance profile at the full design pressure differential of 120 psig while at 1140 °F. Figure 22 shows the commanded (set point) clearance, the control clearance measured by the capacitance probe, and the error between the two signals as a function of time. The maximum error observed between the commanded setpoint clearance and the measured control clearance was an actuator lag of 0.0012 in. The maximum overshoot observed was 0.0007 in. Error was calculated by subtracting the commanded setpoint clearance from the measured control clearance. Using this designation, a negative error on the chart indicates that the clearance set by the ACC system is smaller than the commanded clearance, and a positive error shows that the ACC system has set a clearance larger than the specified value.

This evaluation shows that the ACC concept is capable of tracking an engine clearance transient profile under engine-like temperature and pressure conditions, while maintaining an acceptable level of error. A large portion of the observed error is attributed to a communication lag time between the NI motion controllers and the PC on which the control system software resides. If a dedicated controller was implemented in place of the PC based system used in this laboratory study, the communication lag between the PC and the NI motion controllers would be eliminated. This would likely reduce observed clearance error to less than 0.001 in.

C. Comparison of Effective Clearance to an Industry Reference Level

The benefits of active clearance control are of little importance if the secondary seal leakage associated with the implementation of the ACC system is too large. As such, a practical benchmark, effective clearance (δ_{flow}), was defined to quantify the performance of the ACC test rig and its secondary seals across different builds and varying test conditions, and facilitate a comparison with actual engine requirements. By assuming isentropic flow with compressibility at the choked flow condition, a method for back-calculating effective clearance for the ACC test rig at multiple test conditions was derived (refs. 1 and 9). The equation for determining effective clearance is:

$$\delta_{flow} = \frac{A_{flow}}{C} = \frac{\dot{m}\sqrt{RT}}{0.6847\sqrt{g_c}P_s C} \tag{2}$$

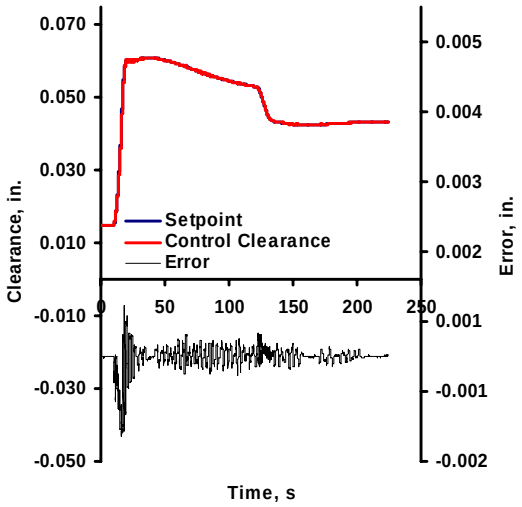

Figure 22.—Simulated flight clearance transient profile and observed tracking error at 120 psig, 1140 °F.

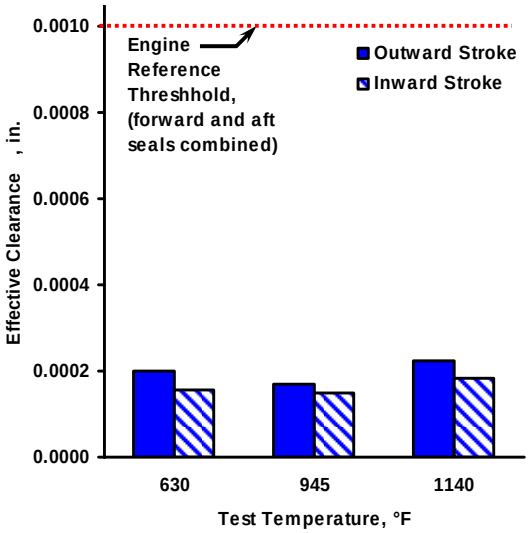

Figure 23.—Comparison of effective clearance at the home position to the engine industry reference threshhold.

To obtain the desired benchmark for comparison, an effective clearance was calculated for a target leakage upper limit specified by industry engine designers. Based on the predicted benefits of tighter HPT blade tip clearances and the proposed location of the ACC system in the engine, designers deemed secondary leakage on the order of ~0.1 percent core flow (W25) an acceptable limit per each seal location. Idealizing the ACC system as an elastic structure that could easily move inward and outward, two seals are needed to integrate the ACC concept into an engine, one on both the forward and aft sides of the seal carriers, placed between the seal carriers and the static structures to which they would be attached. Based on these assumptions, and the industry supplied flow reference level, the maximum allowable effective clearance for the ACC system is 0.0010 in. (ref. 3).

Calculated effective clearance values for representative leakage at the home position (during both an inward and outward stroke) for the three elevated temperatures are presented in figure 23. As shown, all of the calculated effective clearances for these tests were well below the industry reference threshold of 0.0010 in. At a clearance of approximately 0.0002 in., these values are 80 percent lower than the industry goal, about one third lower than the smallest effective clearance observed in previous studies (0.0003 in.), (ref. 3) and show nearly negligible variation with stroke and temperature. These results show that the improvements made to the ACC test rig for this evaluation were indeed effective, and that from a parasitic leakage standpoint, the ACC concept developed at NASA GRC is a very viable technology.

IV. Summary and Conclusions

A new servo-hydraulic actuation system and a redesigned test chamber were integrated into the Active Clearance Control Test Rig at NASA Glenn Research Center to address test limitations imposed by first generation hardware, and extend test capabilities to full design capacity. Tests were conducted to characterize the performance of the new actuators on both an individual and system basis. Static and dynamic leakage of the rig's secondary seal system were evaluated at engine simulated pressures and temperatures up to 120 psig, and 1140°F, respectively, to quantify the improvements gained through the addition of the second generation hardware. During these tests, the following observations were noted:

1. The servo-hydraulic actuators were determined to have a maximum positional error of only 0.0002 in. with a maximum hysteresis error of 0.0001 in. This satisfied the design requirement for an error of less than ±0.0003 in. The new actuators reduced pressure induced deflection of the seal carriers and related hysteresis by approximately 69 percent.

2. Static leakage evaluation at 630, 945, and 1140 °F, showed that secondary seal leakage was consistently lower during an inward stroke of the actuators than during an outward stroke. Examination of flow factor values calculated for static leakages, coupled with trends observed in raw leakage data, showed that leakage variations were not solely the effect of normal gas density effects. This suggested that internal clearances were physically changing as test conditions were varied.
3. For the test conditions evaluated herein, there were no trends observed to suggest that dynamic leakage was significantly different than static leakage at similar temperatures and pressures.
4. The new servo-hydraulic actuation package enabled the ACC system to accurately track a simulated flight clearance transient profile at 1140 °F, 120 psig, with a maximum error of 0.0012 in.
5. Effective clearance values of approximately 0.0002 in. were calculated for leakages at the home position for all three test temperatures. These values are 80 percent lower than the engine industry specified threshold of 0.0010 in., and 33 percent lower than the smallest effective clearance observed in previous evaluations (0.0003 in.) (ref. 3).
6. From the standpoints of control accuracy and secondary seal leakage, the ACC concept evaluated herein is a viable technology that holds significant potential for improving the efficiency of modern gas turbine engines. The ACC test rig is a valuable asset that can be used to evaluate further refinements of the current concept (reduced weight actuators, improved secondary seal technology, etc.), and to examine other clearance control concepts.

References

1. Steinetz, B.M., Lattime, S.B., Taylor, S.C., DeCastro, J.A., Oswald, J.J., Melcher, K.A., "Preliminary Evaluation of an Active Clearance Control System Concept," NASA/TM—2005-213856, AIAA–2005–3989. Presented at the 2005 AIAA/ASME/SAE/ASEE Joint Propulsion Conference, Tucson, AZ.
2. Steinetz, B.M., Taylor, S.C., Oswald, J.J., DeCastro, J.A., "Seal Investigations of an Active Clearance Control System Concept," NASA/TM—2006-214114, 120-ISROMAC-11. Presented at the 11th International Symposium of Rotating Machinery, Honolulu, HI.
3. Taylor, S.C., Steinetz, B. M., Oswald, J.J., "High Temperature Evaluation of an Active Clearance Control Concept," NASA/TM—2006-214464, also AIAA–2006–4750, presented at the AIAA/ASME/SAE/ASEE conference, July, 2006, Sacramento, CA.
4. Halila, E.E., Lenahan, D.T., Thomas, T.T., "Energy Efficient Engine, High Pressure Turbine Test Hardware Detailed Design Report," NASA CR–167955, 1982.
5. Lattime, S.L., Steinetz, B.M., Robbie, M.G., "Test Rig for Evaluating Active Turbine Blade Tip Clearance Control Concepts," *Journal of Propulsion and Power*, vol. 21 (3) May-June 2005, NASA/TM—2003-212533, also AIAA–2003–4700, presented at the AIAA/ASME/SAE/ASEE conference, July, 2003, Huntsville, AL.
6. Lattime, S.L., Steinetz, B.M., "Turbine Engine Clearance Control Systems: Current Practices and Future Directions," *Journal of Propulsion and Power*, vol. 20, no. 2, NASA/TM—2002-211794, also AIAA–2002–3790, presented at the AIAA/ASME/SAE/ASEE conference, July, 2002, Indianapolis, IN.
7. General Electric Aircraft Engines, "HPT Clearance Control (Intelligent Engine Systems)—Phase I—Final Report" NASA Contract NAS3–01135, April 2004.
8. Wiseman, M.W., Guo, T., "An Investigation of Life Extending Control Techniques for Gas Turbine Engines," Proceedings of the American Control Conference, IEEE Service Center, Piscataway, NJ, IEEE Catalog No. 01CH37148, vol. 5, pp. 3706–3707, 2001.
9. Shapiro, Ascher H., The Dynamics and Thermodynamics of Compressible Flow, The Ronald Press Co., New York, 1953.

REPORT DOCUMENTATION PAGE	Form Approved OMB No. 0704-0188

1. REPORT DATE *(DD-MM-YYYY)*	2. REPORT TYPE	3. DATES COVERED *(From - To)*
01-12-2007	Technical Memorandum	

4. TITLE AND SUBTITLE
Further Characterization of an Active Clearance Control Concept

5a. CONTRACT NUMBER

5b. GRANT NUMBER

5c. PROGRAM ELEMENT NUMBER

6. AUTHOR(S)
Taylor, Shawn, C.; Steinetz, Bruce, M.; Oswald, Jay, J.

5d. PROJECT NUMBER

5e. TASK NUMBER

5f. WORK UNIT NUMBER
WBS 984754.02.07.03.13.06

7. PERFORMING ORGANIZATION NAME(S) AND ADDRESS(ES)
National Aeronautics and Space Administration
John H. Glenn Research Center at Lewis Field
Cleveland, Ohio 44135-3191

8. PERFORMING ORGANIZATION REPORT NUMBER
E-16213

9. SPONSORING/MONITORING AGENCY NAME(S) AND ADDRESS(ES)
National Aeronautics and Space Administration
Washington, DC 20546-0001

10. SPONSORING/MONITORS ACRONYM(S)
NASA

11. SPONSORING/MONITORING REPORT NUMBER
NASA/TM-2007-215039; AIAA-2007-5739

12. DISTRIBUTION/AVAILABILITY STATEMENT
Unclassified-Unlimited
Subject Category: 37
Available electronically at http://gltrs.grc.nasa.gov
This publication is available from the NASA Center for AeroSpace Information, 301-621-0390

13. SUPPLEMENTARY NOTES

14. ABSTRACT
A new test chamber and precision hydraulic actuation system were incorporated into an active clearance control (ACC) test rig at NASA Glenn Research Center. Using the improved system, a fast-acting, mechanically-actuated, ACC concept was evaluated at engine simulated temperatures and pressure differentials up to 1140 °F and 120 psig, on the basis of secondary seal leakage and kinematic controllability. During testing, the ACC concept tracked a simulated flight clearance transient profile at 1140 °F, 120 psig, with a maximum error of only 0.0012 in. Comparison of average dynamic leakage of the system with average static leakage did not show significant differences between the two operating conditions. Calculated effective clearance values for the rig were approximately 0.0002 in. at 120 psig, well below the industry specified effective clearance threshold of 0.001 in.

15. SUBJECT TERMS
Active clearance control; Turbine blades; Gas turbine engines; Temperature

16. SECURITY CLASSIFICATION OF:			17. LIMITATION OF ABSTRACT	18. NUMBER OF PAGES	19a. NAME OF RESPONSIBLE PERSON
a. REPORT	b. ABSTRACT	c. THIS PAGE			STI Help Desk (email:help@sti.nasa.gov)
U	U	U	UU	23	19b. TELEPHONE NUMBER *(include area code)* 301-621-0390